Journal of Simulation and Analysis of Novel Technologies in Mechanical Engineering
13 (3) (2021) 0005~0012
HTTP://JSME.IAUKHSH.AC.IR

An agglomerate model for evaluating the electrochemical and hydrodynamic characteristics of a proton exchange membrane fuel cell

Pouya Barnoon, Davood Toghraie*, Babak Mehmandoust, Mohammad Ali Fazilati, S. Ali Eftekhari

Department of Mechanical Engineering, Khomeinishahr Branch, Islamic Azad University, Khomeinishahr, 84175-119, Iran

*Toghraee@iaukhsh.ac.ir

(Manuscript Received --- 30 Jun. 2021; Revised --- 05 Jul. 2021; Accepted --- 6 Jul. 2021)

Abstract

In this article, PEM fuel cell's electrochemical and hydrodynamic characteristics are investigated using an agglomerate model. Modeling is single-phase, two-dimensional, incompressible and steady-state. In this article, current density, water distribution and gas velocity inside the anode and cathode gas diffusion layers are obtained. This study using the present agglomerate model can provide a good prediction of the current density. The results show that the highest current density occurs in the interface areas between current collectors and gas diffusion layers. In addition, there is the highest flow velocity in the sharp areas, where the interface is between the current collectors and the gas diffusion layers. In these areas, values of velocity gradients can affect cell performance. Therefore, in order to achieve better performance, it is necessary to design different flow channels and gas diffusion layers and compare them with each other. Furthermore, the amount of water in the gas diffusion layer should be controlled to not reduce the chemical reaction on the cathode side.

Keywords: Agglomerate, Fuel cell, Electrochemical, Hydrodynamic, PEM.

1-Introduction

Hydrogen is one of the cleanest fuels used in fuel cells today to generate electricity [1]. A fuel cell is a machine that produces electricity through a chemical reaction. All fuel cells have two electrical poles called anodes and cathodes. Chemical reactions take place in these electrodes, leading to the generation of electricity. In addition, each cell has a membrane and two catalyst layers; the role of the electrolyte is to move charged particles between the electrodes, while the catalyst speeds up the reactions at the electrodes [2-4]. In a fuel cell, oxygen enters the cathode and reacts with electrons entering the external circuit and ions transferred from the electrolyte. [5]. The proton exchange membrane fuel cell (PEMFC) works with a polymer electrolyte in a thin, permeable plate. Its efficiency is 40 to 50 percent, its operating temperature is about 80 degrees Celsius and its output power is usually between 50 to 250 kilowatts. The solid and flexible electrolyte of these cells does not leak and does not

crack. Although low operating temperatures have made PEM cells suitable for home and in-car applications, their fuel must be refined and two platinum electrodes placed on either side of the membrane, increasing the cost of manufacturing [6]. Xing [7] studied a mathematical model for a typical PEM fuel cell operated with non-precious carbon-based materials as ORR catalysts. His results showed significance of reactant transport within the carbon agglomerates, indicating primary pores' vital role for reactant transport and cell performance. Molaeimanesh and Akbari [8] studied the cathode catalyst layer modeling of a fuel cell using LBM. They investigated species dissolution and diffusion in electrolyte film and electrochemical reaction and active approach for species transport. They found that non-uniform arrangement was lead to non-homogenous species distribution. Das et al. [9] presented an agglomerate model for the cathode catalyst layer of PEM fuel cells. In their work, a finite element technique was used for the numerical solution to the model developed. In their study, three various arrangements of agglomerates were carried out, an in-line and two staggered. Their results showed that the least overpotential is obtained when an in-line arrangement is considered. Zhang et al. [10] investigated spherical agglomerate models in the catalyst layer to evaluate their reliability. Their technique was providing an improved method to estimate the electrochemical reaction rate in the catalyst layer. They showed that the diameter in the agglomerate model was just a fitting parameter increasing with overpotential. Wang et al. [11] investigated the structure and performance of different types of agglomerates in cathode catalyst layers of PEM fuel cells. In their work, two different agglomerates were analyzed with the aim of identifying current limiting factors. Their results showed that proton penetration depths in water-flooded agglomerates could be quite substantial under certain conditions, resulting in unexpectedly high catalyst utilisation. Zhang et al. [12] developed a new agglomerate model to express the oxygen reduction reaction to calculate the agglomerate model parameters. A parametric study on a fuel cell with agglomerate model was expressed by Machado et al. [13]. They considered the influences of relative humidity, Pt loading and ionomer volume fraction. They found that increasing the performance of the fuel cell was possible by reducing the relative humidity on the cathode side. Yang et al. [14] investigated the behavior of catalyst layer and liquid water transport in a PEM fuel cell using an agglomerate model. Considering the liquid water transfer based on the agglomerate model, a CFD model was used to describe the main structure and parameters of the PEM fuel cell. In their work, an acceptable overlap between experimental and numerical data was observed. Baca et al. [15] performed a three-dimensional analysis to evaluate the power density of a fuel cell at different operating conditions using the CFD method. Their results showed that there is always a non-uniform distribution of current density in the catalyst layer and in all conditions. For further studying, references [24-31] are recommended.

Based on the literature review, it can be concluded that although useful research has been done in the field of catalyst layer (CL) and PEM fuel cell modeling using the agglomerate model. However, as can be seen, there are few studies that consider both hydrodynamic and electrochemical

characteristics using the agglomerate model. In this article, a numerical study on the PEM fuel cell's electrochemical and hydrodynamic characteristics is carried out using an agglomerate model.

2-Problem statement

In this article, two characteristics of the agglomerate model, namely the agglomerate radius and the thickness of the active layer on the polarisation curve, are investigated. Fig. 1 shows a schematic of the problem. According to Fig. 1, the geometry has two parallel channels which is common in fuel cells. The computational domain consists of three main components: anode (Ω_a), cathode (Ω_c), and membrane (Ω_m).

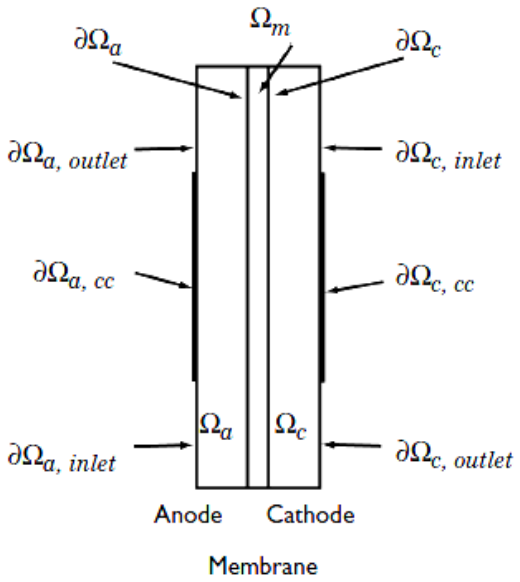

Fig. 1 Schematic of the present problem.

Each electrode consists of an inlet, an outlet and a current collector ($\partial\Omega_a$, cc and $\partial\Omega_c$, cc). Humidified hydrogen enters from the anode ($\partial\Omega_{a,\ inlet}$) and exits the anode after the reaction ($\partial\Omega_{a,\ outlet}$). Air is injected at the cathode side ($\partial\Omega_{c,\ inlet}$) and reacts with protons transferred from the membrane (due to the hydrogen decomposition reaction) and eventually leaves the cathode ($\partial\Omega_{c,\ outlet}$). Therefore, the chemical reaction that occurs in the anode is as follows,

$$H_2 + 2\lambda_{H_2O}H_2O \rightarrow 2\left(H^+ + \lambda_{H_2O}H_2O\right) + 2e^- \quad (1)$$

The chemical reaction that occurs in the cathode is as follows,

$$O_2 + 4\left(H^+ + \lambda_{H_2O}H_2O\right) + 4e^- \rightarrow \left(2 + 4\lambda_{H_2O}\right)H_2O \quad (2)$$

This study assumes that humidified gases on both sides of the anode and cathode behave like ideal gases and are continuous. The electrodes are also considered to be porous and homogeneous. Darcy's law is therefore sufficient to describe the flow in a porous medium. The agglomerate model can also express chemical reactions in catalyst layers [16-19].

3-Governing equations and boundary conditions

The current density expression for both sides is expressed as follows [18],

$$i_e = l_{act}\left(1-\varepsilon_{max}\right) j_{agg,e} \quad (3)$$

where the index e can represent the anode (a) or the cathode (c). The local current density concerning the diffusion equation and the Butler-Volmer equation can be expressed as follows,

$$j_{agg,e} = 6n_eF\left(\frac{D_{agg}}{r_{agg}^2}\right)\left(1-\lambda_e coth\lambda_e\right)\beta_e \quad (4)$$

where [18],

$$\lambda_a = \sqrt{\frac{i_{0,a}Sr_{agg}^2}{2Fc_{H_{2,ref}}D_{agg}}} \quad (5)$$

$$\lambda_c = \sqrt{\frac{i_{0,c}Sr_{agg}^2}{4Fc_{O_{2,ref}}D_{agg}}exp\left(-\frac{F}{2RT}\eta\right)} \quad (6)$$

$$\beta_a = \left[c_{H_{2,agg}} - c_{H_{2,ref}} exp\left(-\frac{2F}{RT}\eta_a \right) \right] \quad (7)$$

$$\beta_c = c_{O_{2,agg}} \quad (8)$$

The overvoltages at both sides (anode and cathode) are written as follows,

$$\eta_a = \phi_s - \phi_s - E_{eq,a} \quad (9)$$

$$\eta_c = \phi_s - \phi_s - E_{eq,c} \quad (10)$$

where E_{eq} denotes the equilibrium voltage. The concentration of species at the surface of agglomerates can be expressed as follows:

$$c_{H_{2,agg}} = \frac{P_{H_2} x_{H_2}}{H_{H_2}} \quad (11)$$

$$c_{O_{2,agg}} = \frac{P_{O_2} x_{O_2}}{H_{O_2}} \quad (12)$$

At the anode the voltage is zero and at the cathode the voltage is equal to the cell voltage, which is expressed as follows,

$$\phi_s = 0 \quad at \quad \partial\Omega_{a,cc} \quad (13)$$

$$\phi_s = 0 \quad at \quad \partial\Omega_{a,cc} \quad (14)$$

The continuity equation is defined as follows [20,21],

$$\vec{\nabla}\left(\rho\vec{u}\right) = 0 \quad (15)$$

Darcy's law is used to express the velocity of flow inside the porous medium as follows [22,23],

$$u = -\frac{K}{\mu}\nabla P \quad (16)$$

According to the ideal gas law, density is calculated as follows:

$$\rho = \frac{P}{RT}\sum_i M_i x_i \quad (17)$$

At the inlets and outlets:

$$P = P_{a,in} \quad at \quad \partial\Omega_{a,inlet} \quad (18a)$$

$$P = P_{ref} \quad at \quad \partial\Omega_{a,outlet} \quad (18b)$$

$$P = P_{c,in} \quad at \quad \partial\Omega_{c,inlet} \quad (18c)$$

$$P = P_{ref} \quad at \quad \partial\Omega_{c,outlet} \quad (18d)$$

Using Faraday's law at the electrode boundary, a phrase for gas velocity can be written as follows,

$$-n.u\big|_{anode} = \frac{j_{agg,a}}{\rho F}\left(\frac{1}{2} M_{H_2} + \lambda_{H_2O} M_{H_2O} \right) \quad (19)$$

$$-n.u\big|_{cathode} = \frac{j_{agg,c}}{\rho F}\left(\frac{1}{2} M_{O_2} + \left(\frac{1}{2} + \lambda_{H_2O} \right) M_{H_2O} \right) \quad (20)$$

There are two species in the anode (H_2 and H_2O) and three species at the cathode (O_2, H_2O, and N_2). Therefore, the mass transfer according to Maxwell-Stefan equation is expressed as follows,

$$\vec{\nabla}.\left[-\rho\omega_i \sum_{j=1}^{N} D_{i,j} \left\{ \frac{M}{M_j}\left(\vec{\nabla}\omega_j + \omega_j \frac{\nabla M}{M} \right) = \left(x_j - \omega_j \right)\frac{\vec{\nabla}P}{P} \right\} + \omega_j \rho u \right] = R_i \quad (21)$$

Assuming that O_2=1, H_2O=2 and N_2=3, the following equations are used to describe the fluid flow,

$$-\vec{\nabla}.\left[-\rho\omega_1 \sum_j D_{1,j}\left(\vec{\nabla}\omega_j + \omega_j \frac{\nabla M}{M} \right) + \left(x_j - \omega_j \right)\frac{\vec{\nabla}P}{P} \right] = -\left(\rho u.\nabla\omega_1 \right) \quad (22)$$

$$-\vec{\nabla}.\left[-\rho\omega_2\sum_j D_{2,j}\left(\vec{\nabla}\omega_j+\omega_j\frac{\nabla M}{M}\right)+\left(x_j-\omega_j\right)\frac{\vec{\nabla}P}{P}\right]=-\left(\rho u.\nabla\omega_2\right) \quad (23)$$

$$\omega_3=1-\omega_1-\omega_2 \quad (24)$$

The mass fractions of the species are known at the inlets and the convective flux is specific at the outlets. At the interface between the membrane and the electrode, according to the reaction rate, the boundary conditions are written as follows:

$$-n.N_{H_2}\Big|_{anode}=\frac{j_{anode}}{2F}M_{H_2} \quad (25)$$

$$-n.N_{O_2}\Big|_{cathode}=\frac{j_{cathode}}{4F}M_{O_2} \quad (26)$$

$$-n.N_{H_2O}\Big|_{cathode}=\frac{j_{cathode}}{F}\left(\frac{1}{2}+\lambda_{H_2O}\right)M_{H_2O} \quad (27)$$

4-Results and discussion

Fig. 2 depicts the current density at the anode and cathode sides. As can be seen, the amount of current density in the vicinity of the current collectors is maximum.

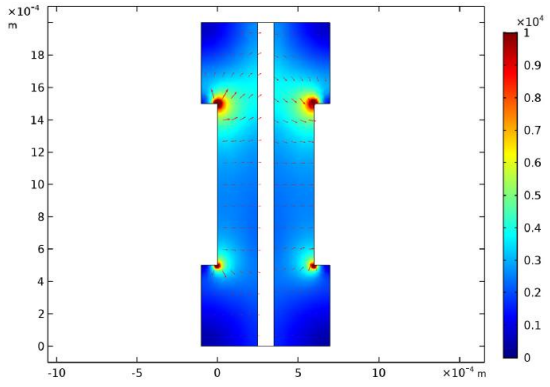

Fig. 2 Current density contour and current vector at 0.7 V.

To better understand how the current density changes, the current density diagram and the anode side in terms of cell height is plotted in Fig. 3. The maximum and minimum current densities are for the outlet and inlet areas, respectively. The reaction rate on the cathode side can affect the current density distribution on the anode side. At the cathode side, the opposite is true, meaning that the maximum current density occurs at the cathode inlet regions.

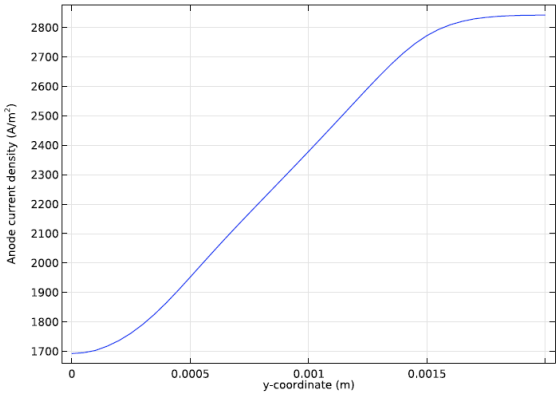

Fig. 3 Current density variation at the active layer

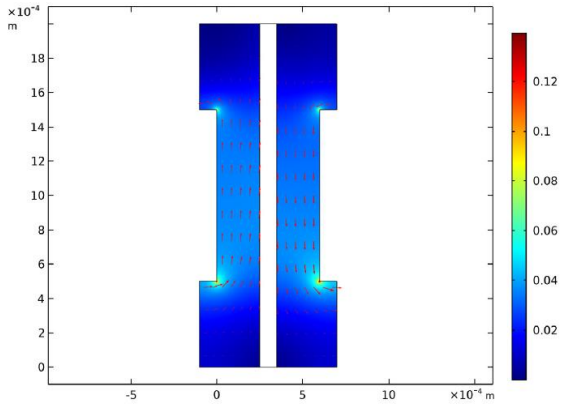

Fig. 4 Gas velocity contour in the gas diffusion layers.

Fig. 4 depicts the flow rate contour in the gas diffusion layers. As can be seen, the highest velocity is observed in the areas closest to the current collectors (where the highest current density is present).

Fig. 5 depicts the mass fractions of the species at the cathode and anode sides. It is observed that the mass fraction of oxygen decreases as it progresses in the cathode

channel, but the mass fraction of the hydrogen increases as it progresses in the anode channel, which is due to the electroosmotic drag of water through the electrolyte, which can lead to higher flux than consumption of hydrogen. It should be noted that although oxygen consumption is low, overvoltage concentration in agglomerates can have a significant effect on overvoltage concentration, so that for small changes in the amount of oxygen flow, significant changes can be observed in the polarisation curve.

Fig. 6 depicts the contour of the water distribution at the anode and cathode sides. It is observed that the water is transferred to the anode by the mechanism of convective and diffusion. The presence of water in keeping the membranes and gases moist is essential for easy ionic conductivity. On the cathode side, water rises at the outlet. Therefore, the water must be appropriately controlled to prevent a chemical reaction on the cathode side.

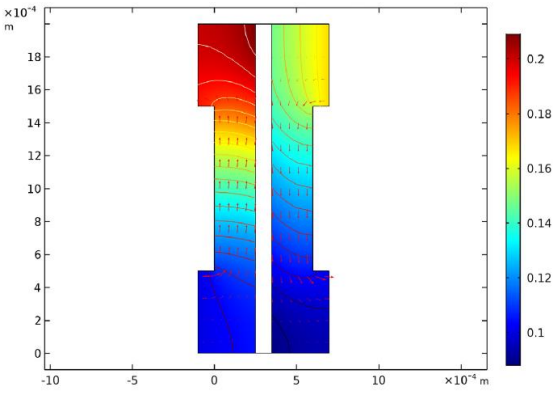

Fig. 5 Mass fractions of species and Darcy's velocity vector at the anode and cathode sides.

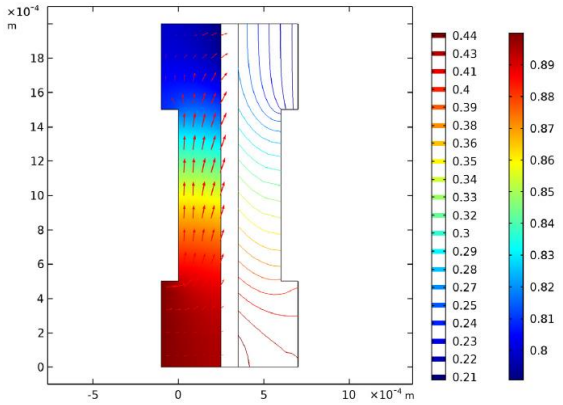

Fig. 6 Mass fraction of water in the gas diffusion layers.

5-Conclusion

In this article, the characteristics of a PEM fuel cell were studied using the agglomerate model. The cathode is an important member in the fuel cell and by changing the amount of current in that part, the performance of the cell in general is affected. Minimal water occurs in the areas upstream of the anode. Moisturizing gases is essential for the reaction and can affect ionic conductivity. Most of the flow velocity occurs in the sharp (current collector) areas. Therefore, since flow velocity can affect performance, cell performance can be improved by different designs for flow channels and gas diffusion layers.

References

[1] Barnoon, P., Toghraie, D., Mehmandoust, B., Fazilati, M. A., & Eftekhari, S. A. (2021). Comprehensive study on hydrogen production via propane steam reforming inside a reactor. *Energy Reports*, *7*, 929-941.

[2] Baschuk, J. J., & Li, X. (2000). Modelling of polymer electrolyte membrane fuel cells with variable degrees of water flooding. *Journal of power sources*, *86*(1-2), 181-196.

[3] Meng, H. (2007). A two-phase non-isothermal mixed-domain PEM fuel cell model and its application to two-dimensional simulations. *Journal of Power Sources*, *168*(1), 218-228.

[4] Das, P. K., Li, X., & Liu, Z. S. (2010). Analysis of liquid water transport in cathode catalyst layer of PEM fuel cells. *International Journal of Hydrogen Energy*, *35*(6), 2403-2416.

[5] Leo, T. J., Durango, J. A., & Navarro, E. (2010). Exergy analysis of PEM fuel cells for marine applications. *Energy*, *35*(2), 1164-1171.

[6] Kim, J. Y., Oh, T. K., Shin, Y., Bonnett, J., & Weil, K. S. (2011). A novel non-platinum group electrocatalyst for PEM fuel cell application. *International journal of hydrogen energy*, *36*(7), 4557-4564.

[7] Xing, L. (2018). An agglomerate model for PEM fuel cells operated with non-precious carbon-based ORR catalysts. *Chemical Engineering Science*, *179*, 198-213.

[8] Molaeimanesh, G. R., & Akbari, M. H. (2015). Agglomerate modeling of cathode catalyst layer of a PEM fuel cell by the lattice Boltzmann method. *International Journal of Hydrogen Energy*, *40*(15), 5169-5185.

[9] Das, P. K., Li, X., & Liu, Z. S. (2008). A three-dimensional agglomerate model for the cathode catalyst layer of PEM fuel cells. *Journal of Power Sources*, *179*(1), 186-199.

[10] Zhang, X., Ostadi, H., Jiang, K., & Chen, R. (2014). Reliability of the spherical agglomerate models for catalyst layer in polymer electrolyte membrane fuel cells. *Electrochimica Acta*, *133*, 475-483.

[11] Wang, Q., Eikerling, M., Song, D., & Liu, Z. (2004). Structure and performance of different types of agglomerates in cathode catalyst layers of PEM fuel cells. *Journal of Electroanalytical Chemistry*, *573*(1), 61-69.

[12] Zhang, X., Gao, Y., Ostadi, H., Jiang, K., & Chen, R. (2014). A proposed agglomerate model for oxygen reduction in the catalyst layer of proton exchange membrane fuel cells. *Electrochimica Acta*, *150*, 320-328.

[13] Machado, B. S., Mamlouk, M., & Chakraborty, N. (2019). Three-dimensional agglomerate model of an anion exchange membrane fuel cell using air at the cathode–A parametric study. *Journal of Power Sources*, *412*, 105-117.

[14] Jung, C. Y., Park, C. H., Lee, Y. M., Kim, W. J., & Yi, S. C. (2010). Numerical analysis of catalyst agglomerates and liquid water transport in proton exchange membrane fuel cells. *International journal of hydrogen energy*, *35*(16), 8433-8445.

[15] Baca, C. M., Travis, R., & Bang, M. (2008). Three-dimensional, single-phase, non-isothermal CFD model of a PEM fuel cell. *Journal of Power Sources*, *178*(1), 269-281.

[16] Scott, H. F. (2016). *Elements of chemical reaction engineering*. Prentice Hall.

[17] Bird, R. B., Stewart, W. E., & Lightfoot, E. N. (2006). *Transport phenomena* (Vol. 1). John Wiley & Sons.

[18] Broka, K., & Ekdunge, P. (1997). Modelling the PEM fuel cell cathode. *Journal of Applied Electrochemistry*, *27*(3), 281-289.

[19] Dannenberg, K., Ekdunge, P., & Lindbergh, G. (2000). Mathematical model

of the PEMFC. *Journal of Applied Electrochemistry*, *30*(12), 1377-1387.

[20] Barnoon, P., & Ashkiyan, M. (2020). Magnetic field generation due to the microwaves by an antenna connected to a power supply to destroy damaged tissue in the liver considering heat control. *Journal of Magnetism and Magnetic Materials*, *513*, 167245.

[21] Shahsavar, A., Entezari, S., Toghraie, D., & Barnoon, P. (2020). Effects of the porous medium and water-silver biological nanofluid on the performance of a newly designed heat sink by using first and second laws of thermodynamics. *Chinese Journal of Chemical Engineering*, *28*(11), 2928-2937.

[22] Shahsavar, A., Noori, S., Toghraie, D., & Barnoon, P. (2021). Free convection of non-Newtonian nanofluid flow inside an eccentric annulus from the point of view of first-law and second-law of thermodynamics. *ZAMM-Journal of Applied Mathematics and Mechanics/Zeitschrift für Angewandte Mathematik und Mechanik*, *101*(5).

[23] Barnoon, P., Toghraie, D., Salarnia, M., & Karimipour, A. (2020). Mixed thermomagnetic convection of ferrofluid in a porous cavity equipped with rotating cylinders: LTE and LTNE models. *Journal of Thermal Analysis and Calorimetry*, 1-40.

[24] Nguyen, Q., Naghieh, A., Kalbasi, R., Akbari, M., Karimipour, A., & Tlili, I. (2021). Efficacy of incorporating PCMs into the commercial wall on the energy-saving annual thermal analysis. *Journal of Thermal Analysis and Calorimetry*, *143*(3), 2179-2187.

[25] Chen, Z., Akbari, M., Forouharmanesh, F., Keshani, M., Akbari, M., Afrand, M., & Karimipour, A. (2020). A new correlation for predicting the thermal conductivity of liquid refrigerants. *Journal of Thermal Analysis and Calorimetry*, 1-6.

[26] Parsian, A., & Akbari, M. (2018). New experimental correlation for the thermal conductivity of ethylene glycol containing Al 2 O 3–Cu hybrid nanoparticles. *Journal of Thermal Analysis and Calorimetry*, *131*(2), 1605-1613.

[27] Delshekasteh, N., & Kolahdooz, A. (2019). Statistical Approach on Microstructure and Hardness of Semi-Solid Cast Aluminum Alloy A380 Produced by Mechanical Vibration in Argon Gas Atmosphere. *Founding Research Journal*, *2*(4), 275-286.

[28] Kolahdooz, A. (2019). Investigation of the hardness improvement for Al-A380 alloy using the controlled atmosphere in the mechanical stirring casting method. *Proceedings of the Institution of Mechanical Engineers, Part E: Journal of Process Mechanical Engineering*, *233*(2), 225-233.

[29] Kolahdooz, A., & Latifi Rostami, S. A. (2018). Experimental and FEM Analysis of Ribs Defects on Composite Lattice Cylindrical Shells. *Journal of Modern Processes in Manufacturing and Production*, *7*(3), 5-18.

[30] Gholami, O., Shakeri, M., Imen, S. J., & Jamshidi Aval, H. (2021). Small-scale resistance seam welding of stainless steel bipolar plates of PEM fuel cells. *International Journal of Energy Research*.

[31] Vazifeshenas, Y., Sedighi, K., & Shakeri, M. (2020). Open Cell Metal Foam as Extended Coolant Surface–Fuel Cell Application. *Fuel Cells*, *20*(2), 108-115.